

# Conversion–Temperature–Property Relationships in Thermosetting Systems: Property Hysteresis Due to Microcracking of an Epoxy/Amine Thermoset–Glass Fiber Composite

AMY S. VALLELY, JOHN K. GILLHAM

Department of Chemical Engineering, Princeton University, Princeton, New Jersey 08544

Received 3 June 1996; accepted 29 July 1996

**ABSTRACT:** A single specimen of an epoxy/amine thermoset–glass fiber composite was examined, using a freely oscillating torsion pendulum operating at  $\sim 1$  Hz, for different conversions (as measured by  $T_g$ ) from  $T_{g0} = 0^\circ\text{C}$  to  $T_{g\infty} = 184^\circ\text{C}$  during cooling and heating temperature scans.  $T_g$  was increased for successive pairs of scans by heating to higher and higher temperatures. The data were used in two ways: (i) vs. temperature for a fixed conversion to obtain transitions, modulus, and mechanical loss data, and (ii) by crossplotting to obtain isothermal values of the mechanical parameters vs. conversion ( $T_g$ ). Hysteresis between cooling and subsequent heating data was observed in temperature scans of essentially ungelled material ( $T_g < 70^\circ\text{C}$ ) and was attributed to spontaneous microcracking. Hysteresis was analyzed in terms of the following three parameters:  $T_{\text{crack}}$ , the temperature corresponding to the onset of microcracking on cooling;  $T_{\text{heal}}$ , the temperature at which the specimen heals on subsequent heating; and the difference between isothermal cooling and heating data vs. conversion. Results were incorporated into a more general conversion–temperature–property diagram which serves as a framework for relating transitions (relaxations) to macroscopic behavior. © 1997 John Wiley & Sons, Inc. *J Appl Polym Sci* **64**: 39–53, 1997

## INTRODUCTION

The overall goal of this group's research is the understanding of the evolution of properties with increased cure in thermosetting polymers. Such research is crucial to the design of reinforced thermosets to replace metals since, e.g., optimum properties do not necessarily correspond to full cure. Examination of isothermal modulus vs. conversion data has revealed an "anomaly," where the isothermal modulus decreases with increasing cure. This anomaly has also been observed in other properties such as density at  $25^\circ\text{C}$ , water absorption at  $25^\circ\text{C}$ , and free volume at  $25^\circ\text{C}$ .<sup>1</sup> One

of the major defects of thermosetting network glasses is their inherent brittleness. This article studies the consequences of the generation and healing of microcracks on the dynamic mechanical behavior of an epoxy/amine thermoset–glass fiber composite specimen, as well as further aspects of the anomaly. The particular specimen is appropriate since fiber-reinforced structures are important applications of high-performance cross-linked thermosets. Microcracking is assumed to arise on cooling as a consequence of the mismatch in the coefficients of thermal contraction of the organic matrix material and the inorganic glass filament reinforcement of the specimen. Dynamic mechanical measurements reveal hysteresis between cooling and subsequent heating data which is attributed to the microcracking. This work

Correspondence to: J. K. Gillham.

© 1997 John Wiley & Sons, Inc. CCC 0021-8995/97/010039-15

formed part of a BSE thesis.<sup>2</sup> Previous work on hysteresis and microcracking has been investigated on a different chemical system.<sup>3</sup> Previous work on the anomaly has involved various thermosetting systems including that used for the present report.<sup>1,4-9</sup>

## EXPERIMENTAL

A single composite specimen of a diepoxy (diglycidyl ether of bisphenol-A, "DGEBA," DER-332 from Dow Chemical Co.) with a balanced stoichiometric amount of an aromatic tetrafunctional diamine (trimethylene glycol di-*p*-aminobenzoate, "TMAB," Versalink from Air Products Co.) on a glass fiber braid substrate was examined using torsional braid analysis (TBA).<sup>1</sup> The TBA unit is a freely oscillating torsion pendulum with frequency  $\approx 1$  Hz. A review of the technique and its application to thermosetting systems has recently been published.<sup>1</sup> The specimen was  $\sim 50$  mm in length and  $\sim 0.5$  mm in diameter, with  $\sim 25$  mg of the reactive epoxy/amine mixture. Use of a single specimen for all experiments provides an internal reference: For a given  $T_g$ , data are remarkably reproducible, and data vs. conversion ( $T_g$ ) vary systematically with little scatter. (In contrast, data from multiple specimens are not reproducible due to problems associated with mounting and aligning the specimens and the ratio of epoxy/amine mixture to glass fiber differing from specimen to specimen.) Transition temperatures were assigned from the maxima in the logarithmic data vs. temperature obtained during cooling. The relative rigidity parameter ( $=f^2$ , where  $f$  is the frequency) is proportional to the relative modulus of the specimen in the absence of dimensional

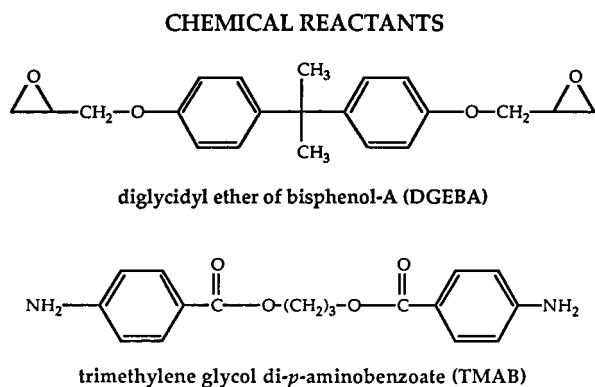


**Figure 1** Chemical reactants.

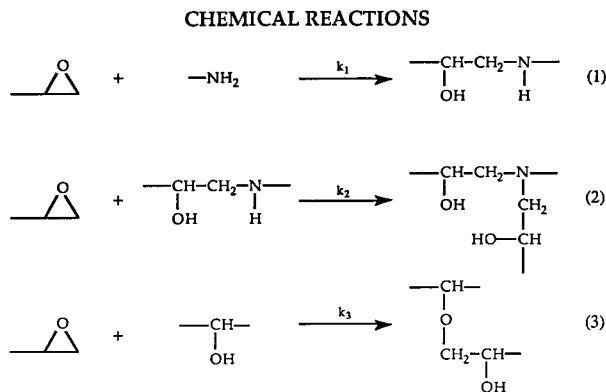


**Figure 2** Reactions of the crosslinking system ( $k_1$ ,  $k_2$ , and  $k_3$  are the rate constants). Reactions (1) and (2) are dominant in the balanced stoichiometric DGEBA/TMAB system ( $k_1 \approx k_2 \gg k_3$ ).

changes.<sup>1</sup> The logarithmic parameter ( $\Delta$ ) is proportional to  $\tan \delta$  ( $\delta \equiv$  phase angle between stress and strain) of the specimen.

Chemical reactants are shown in Figure 1; the chemical reactions of the epoxy/amine system are shown in Figure 2. Schematic network structures at partial cure and full cure, respectively, are shown in Figures 3 and 4. Assuming that the epoxy/amine reactions dominate and have equal reactivities, the lowest theoretical fractional conversion at "molecular" gelation for a tetrafunctional branching unit would be 0.58, which, from the relationship between  $T_g$  and fractional conversion, corresponds to a glass transition temperature  $_{\text{gel}}T_g = 50^\circ\text{C}$ .<sup>1</sup> Macroscopically observed gelation occurs at a higher conversion corresponding to  $_{\text{gel}}T'_g \approx 70^\circ\text{C}$ .<sup>1</sup> The single specimen, initially unreacted, was heated to successively higher maximum temperatures ( $T_{\text{max}}$ ) to increase conversion (i.e.,  $T_g$ ) incrementally. (In some cases,  $T_{\text{max}}$  was below  $T_g$  [i.e., for  $T_{\text{max}}$  values of 160–175°C], in which case conversion ( $T_g$ ) was assigned the value of  $T_{\text{max}}$  on the basis that vitrification [e.g.,  $T = T_g$ ] reduces the reaction rate significantly. Heating above the glass transition temperature "erases" the effects of physical aging. Thus, when  $T_{\text{max}} < T_g$ , the effects of physical aging are not removed so the modulus and  $T_g$  may be higher than an unaged specimen, but this effect is considered to be small since the time for physical aging is small.<sup>10</sup> (In retrospect, for this report, the experimental procedure should have always had  $T_{\text{max}} > T_g$ .) The specimen was cooled to  $-180^\circ\text{C}$  between successive maximum temperatures before being heated to a higher value of

## STRUCTURE: PARTIAL CURE

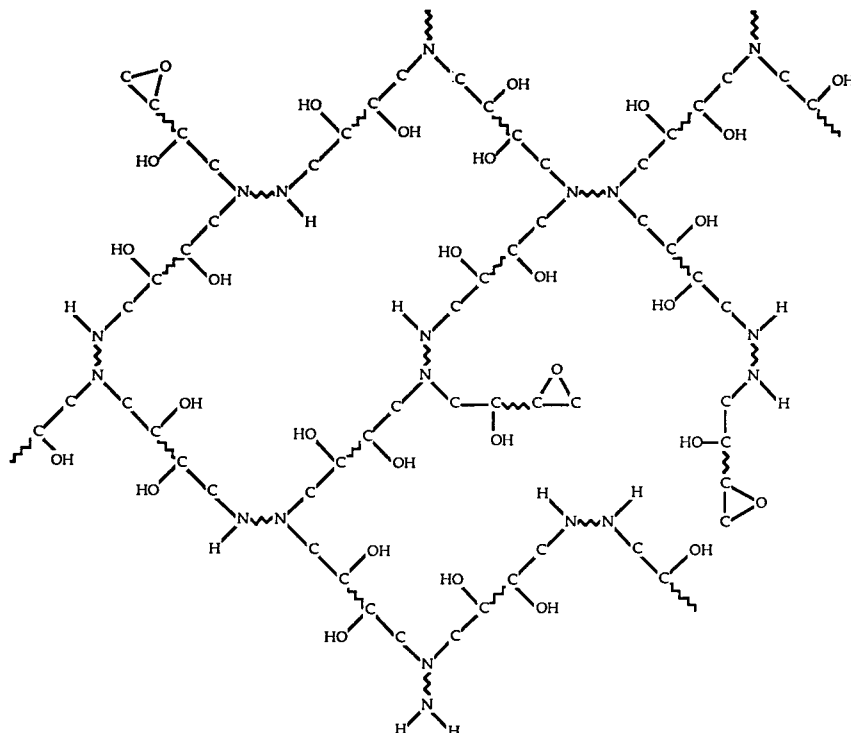


**Figure 3** Schematic crosslinked structure arising from partial cure. Note the presence of epoxide groups and amino hydrogens.

$T_{\max}$ , thereby providing measures of modulus (relative rigidity) and mechanical loss (logarithmic decrement) vs. temperature for both cooling and heating ramps: cooling and heating rates were  $2^{\circ}\text{C}/\text{min}$ . The atmosphere was flowing helium. Figure 5 shows a schematic time–temperature sequence for this procedure. Conversion was measured by the glass transition temperature,  $T_g$ , on the basis of the one-to-one relationship between  $T_g$  and conversion.<sup>1</sup> Crossplotting of the sequential temperature ramping data provided isothermal modulus vs. conversion ( $T_g$ ) data.

## RESULTS AND DISCUSSION

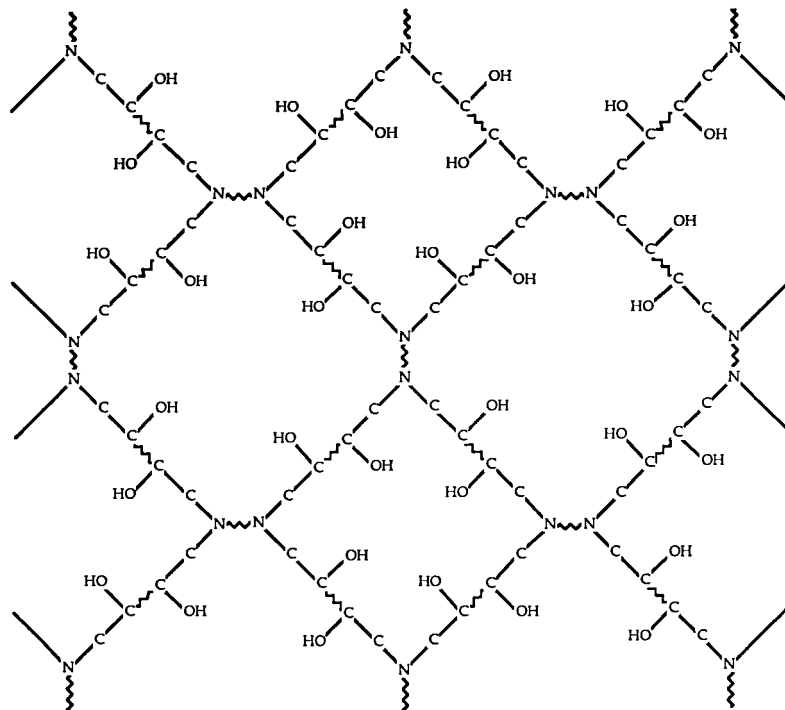
### Evolution of Decreasing Hysteresis in Modulus Between Cooling and Heating with Increasing Conversion

Figure 6 shows the thermomechanical behavior (modulus and mechanical loss) of the single specimen of the DGEBA–TMAB system on cooling from and successive heating to four different max-

imum temperatures for conversions corresponding to  $T_g = 0, 50, 122,$  and  $184^{\circ}\text{C}$ . The most intense peak in each logarithmic decrement spectrum corresponds to  $T_g$ . Vertical arrows mark the following peaks in the logarithmic decrement: the  $\gamma$ -relaxation,  $T_{\gamma}$ , and the liquid–liquid transition,  $T_{ll}$ , on the  $T_g = 0^{\circ}\text{C}$  curve, and the  $\beta$ -relaxation,  $T_{\beta}$ , and the glass transition,  $T_g$ , on the  $T_g = 184^{\circ}\text{C}$  curve. (The summary diagrams of Figures 16 and 17 include transition temperature values vs. conversion.) Hysteresis between cooling and heating data is especially apparent below  $T_g$  in the modulus (relative rigidity) data and in the mechanical damping (logarithmic decrement) data in Figure 6 for  $T_g = 0^{\circ}\text{C}$  and  $T_g = 50^{\circ}\text{C}$ . Only the modulus data are used herein to analyze the hysteresis.

The onset of microcracking on cooling is defined as the temperature in the glassy state at which the modulus begins to decrease with further cooling (e.g., see  $T_g = 0^{\circ}\text{C}$  and  $T_g = 50^{\circ}\text{C}$  data in Fig. 6). The onset of microcracking on cooling vs. conversion is shown in Figure 7. The temperature of the onset of microcracking on cooling decreases

## STRUCTURE: FULLY CURED



**Figure 4** Schematic crosslinked structure arising from full cure. Note that no chain ends are present. The structure is a single network molecule. An actual material would not have such an ordered structure; ring size would vary throughout the network.

with increased conversion. As the material becomes tougher, greater stress (associated with lower temperature) is required to induce microcracking. No microcracking was observed for conversions greater than that of macroscopic gelation ( $T_g \approx 70^\circ\text{C}$ ).

The healing temperature is defined as the temperature in the glassy state at which the modulus on heating (after prior cooling to  $-180^\circ\text{C}$  and associated microcracking) has "healed" and thus has the same value as the modulus on cooling. Figure 8 shows a plot of the healing temperature vs. conversion. The healing temperature is related to the glass transition temperature: The vitrification line,  $T = T_g$ , is presented for reference. Note that the difference between  $T_g$  and  $T_{\text{heal}}$  appears to be approximately constant ( $\sim 20^\circ\text{C}$ ). The healing temperature may represent the low-temperature side of the glass transition region.

Isothermal modulus vs. conversion data were obtained by crossplotting temperature ramp data from both cooling and subsequent heating runs. All relative rigidity (modulus) data were normalized so that the  $25^\circ\text{C}$  value at full cure was unity.

Figure 9 is an example of an isothermal modulus vs. conversion plot. At low conversions, hysteresis was present between the isothermal modulus vs. conversion data obtained from cooling ramps and the data subsequently obtained from heating ramps: Numerical values of the data obtained from heating ramps were lower than those obtained from prior cooling ramps. In this work, microcracking was considered to occur only on cooling; no additional microcracking was considered to occur during subsequent heating. By comparing the difference spectra (i.e., modulus from cooling ramp *minus* modulus from heating ramp) vs. conversion, three temperature regions of hysteresis (microcracking) behavior were defined (i.e., A, B, and C).

*Region A:*  $T \lesssim -40^\circ\text{C}$ . At very low temperatures, no healing of microcracks occurs on heating from  $-180^\circ\text{C}$  to  $T$ . Thus, the difference between the moduli extracted from cooling and subsequent heating data represents the degree of further microcracking on cooling from  $T$  to  $-180^\circ\text{C}$ . The difference may not represent the total degree of microcracking since the specimen may be already

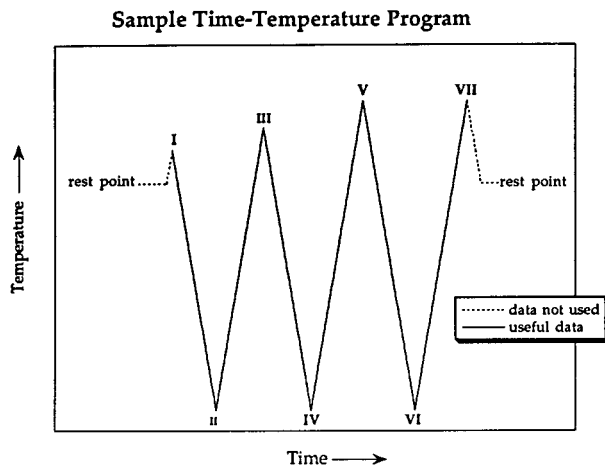


**Figure 5** Sample time-temperature sequence for a TBA experiment. From a rest point, the specimen is heated to I. Point I corresponds to the first  $T_{\max}$  which is above  $T_g$ . From I, the specimen is cooled to II ( $-180^\circ\text{C}$ ) and heated through the first  $T_{\max}$  to point III, the second  $T_{\max}$ . Data from I-II (cooling) and II-III (heating) correspond to the first  $T_{\max}$ . Similarly, III-V corresponds to the second  $T_{\max}$ , and V-VII corresponds to the third  $T_{\max}$ . After VII, which is a temperature equal to or greater than the third  $T_{\max}$ , the specimen is returned to a rest point. Data up from and down to a rest point are not used and are designated with a dashed line in the figure. Limitations of the temperature programmer necessitate the use of rest points. The total experiment consisted of many repetitions of this sample TBA experiment with different values of  $T_{\max}$ .

microcracked when the cooling measurement is attained on cooling from  $T_{\max}$ . Figure 10 shows the degree of further microcracking on cooling to  $-180^\circ\text{C}$  vs. conversion for several isothermal temperatures in Region A. Hysteresis is apparent for low conversions ( $T_g$ ). For low conversions ( $T_g$ ), on heating up from the minimum temperature ( $-180^\circ\text{C}$ ), the modulus represents a microcracked specimen and is thus low. Also, for low conversions, as the isothermal temperature of the modulus measurement increased, the difference between the down and up moduli increased. The larger the temperature difference between the temperature of measurement and the minimum temperature ( $-180^\circ\text{C}$ ), the more microcracking that occurs on cooling below the temperature of measurement. Note that all the difference curves in this region begin with a steep decrease at very low conversions, followed by a more moderate decrease, finally reaching zero difference at  $T_g \approx 70^\circ\text{C}$ . The decrease in hysteresis corresponds to the evolution from brittle to tough material with

increasing conversion. Toughness is associated with gelled material. The theoretical gelation point,  $_{\text{gel}}T_g = 50^\circ\text{C}$ , is marked by a dashed line. Macroscopic gelation occurs at a somewhat higher conversion ( $T_g \approx 70^\circ\text{C}$ ).

**Region B:**  $-40^\circ\text{C} \leq T \leq 20^\circ\text{C}$ . At intermediate temperatures, healing on heating can play a role in the observed hysteresis. Again, the observed hysteresis is measured using the difference between isothermal modulus data extracted from cooling ramps and subsequent heating ramps. Figure 11 shows the observed hysteresis in the isothermal modulus vs. conversion for several isothermal temperatures in Region B. On heating up from  $-180^\circ\text{C}$ , the modulus may represent a microcracked structure, resulting in a difference between the down and up values of the modulus. In Region B, as the isothermal temperature of the modulus measurement increased, the difference between the down and up moduli decreased. This reverse of the trend in Region A is likely due to the proximity of the temperature of measurement to the glass transition temperature which indicates that healing occurs. The initial steep decline in the difference between the down and up moduli is similar to Region A. The conversion corresponding to the local maximum difference increases with increasing isothermal temperature of the measurement. This local maximum is considered to reflect competition between the increased brittleness associated with the increased depth of  $T$  in the glassy state due to the rise in  $T_g$  and increased toughness associated with increased conversion. The curves finally converge to zero difference at  $T_g \approx 70^\circ\text{C}$ , which is similar to Region A. As in Figure 10, the theoretical gelation point,  $_{\text{gel}}T_g = 50^\circ\text{C}$ , is marked by a dashed line.

**Region C:**  $T \leq 20^\circ\text{C}$ . At higher temperatures, hysteresis between data extracted from cooling ramps and subsequent heating ramps was not evident in the isothermal modulus vs. conversion plots; thus, no difference plot is shown. At conversions less than  $T_g \approx 70^\circ\text{C}$ , the specimen is considered to microcrack on cooling to  $-180^\circ\text{C}$ , but to completely heal at a temperature lower than  $T$  on heating. No microcracking is considered to occur on cooling to  $-180^\circ\text{C}$  after material reaches the conversion corresponding to macroscopic gelation,  $T_g \approx 70^\circ\text{C}$ .

Figure 12 shows a compilation of the results on microcracking and hysteresis on the form of a conversion-temperature-hysteresis diagram. This diagram is based on the conversion-temper-

## Thermomechanical Behavior at Different Conversions

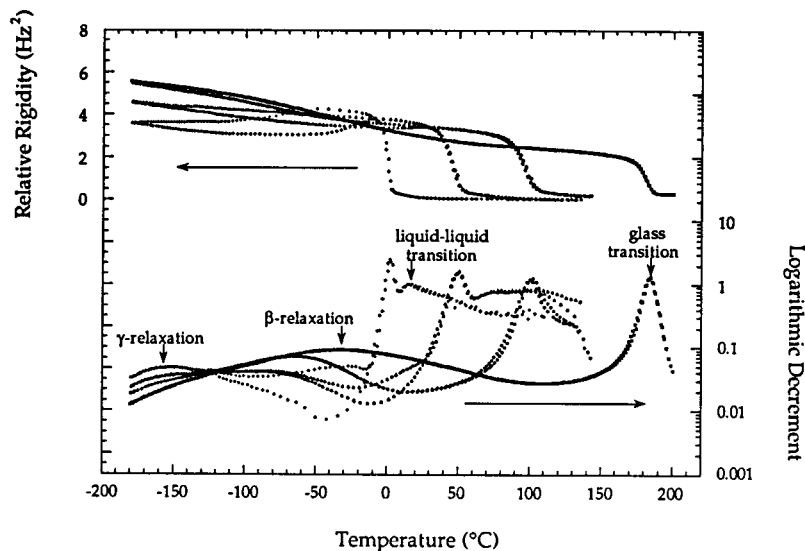


**Figure 6** Thermomechanical behavior of a single specimen of the DGEBA-TMAB system on cooling from and heating to four different maximum temperatures which resulted in the following conversions:  $T_g = 0, 50, 122,$  and  $184^\circ\text{C}$ . The most intense peak in each logarithmic decrement spectrum corresponds to  $T_g$ . Vertical arrows mark the following peaks in the logarithmic decrement: the  $\gamma$ -relaxation,  $T_\gamma$ , and the liquid-liquid transition,  $T_{ll}$ , on the  $T_g = 0^\circ\text{C}$  curve, and the  $\beta$ -relaxation,  $T_\beta$ , and the glass transition,  $T_g$ , on the  $T_g = 184^\circ\text{C}$  spectrum.

ature-property diagram, reports on which have been published.<sup>1,4-6</sup> The region of hysteresis (shaded) is defined by the extrapolated boundaries of the healing temperature on heating ( $T_{\text{heal}}$ ) and the end of hysteresis corresponding to a con-

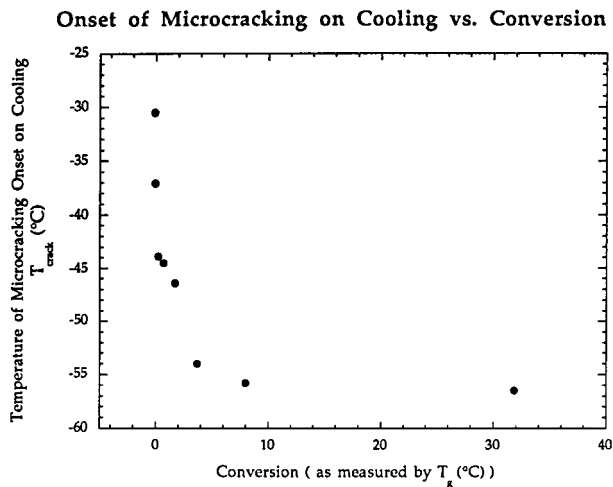


**Figure 7** Onset of microcracking on cooling vs. conversion. The onset of microcracking is defined as the temperature in the glassy state at which the modulus begins to decrease with further cooling.

## Heating Temperature on Heating vs. Conversion

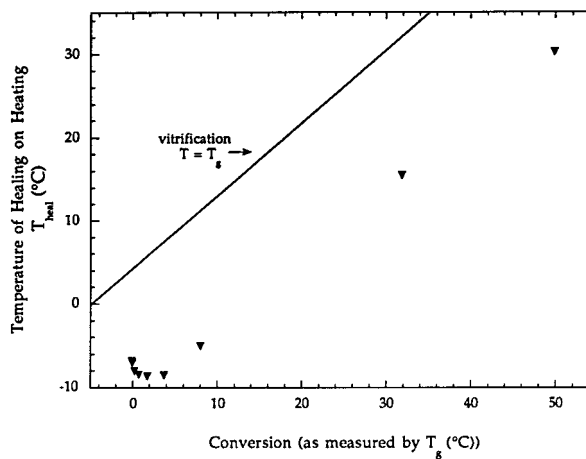


**Figure 8** Healing temperature vs. conversion. The healing temperature is defined as the temperature in the glassy state at which the modulus on heating has "healed" and thus has the same value as the modulus on prior cooling. The healing temperature is related to the glass transition temperature; the vitrification line,  $T = T_g$  is presented for reference.

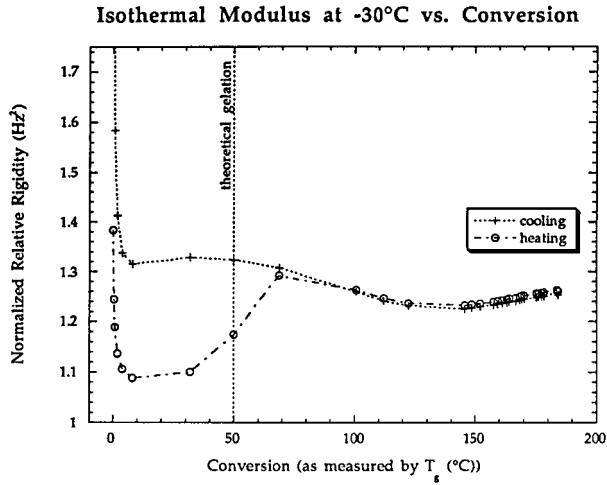


**Figure 9** Isothermal modulus at  $-30^{\circ}\text{C}$  vs. conversion. Data were extracted from sequential (+) cooling and (o) heating ramps. Relative rigidity data were normalized so that the fully cured specimen at  $25^{\circ}\text{C}$  had the value 1. Hysteresis between data extracted from cooling ramps and data extracted from heating ramps presumably arises from microcracking on cooling through  $-30$  to  $-180^{\circ}\text{C}$ . (The lower values obtained from the heating ramps suggest that the specimen microcracked during the cooling ramp.) Note that no hysteresis is present above  $T_g \approx 70^{\circ}\text{C}$ . The dashed vertical line corresponds to theoretical gelation,  $_{\text{gel}}T_g = 50^{\circ}\text{C}$ .

version of  $T_g \approx 70^{\circ}\text{C}$ . The temperature of the onset of microcracking on cooling ( $T_{\text{crack}}$ ) and the maximum in hysteresis are also shown. Note that the temperature of the onset of microcracking on cooling has been extrapolated to drop below  $-180^{\circ}\text{C}$  near  $T_g = 70^{\circ}\text{C}$ , which probably corresponds to macroscopic gelation. It is interesting to consider extrapolation, as in Figure 12, of the maximum in hysteresis data to lower conversions (to the onset of microcracking data) and to higher conversions (to the extrapolated junction of the healing temperature and end of hysteresis data).

### Evolution of Isothermal Modulus and Transitions with Increasing Conversion

Three temperature regions of the isothermal modulus vs. conversion behavior were identified from data extracted from cooling ramps (i.e., I, II and III). At very low temperatures, Region I:  $T \leq -75^{\circ}\text{C}$ , the material is deep in the glassy state for all conversions. Figure 13 shows isothermal modulus data vs. conversion for several different isothermal temperatures in this region. The sharp initial decline in the modulus vs. conversion data at very low conversions has been attributed to

### Degree of Further Microcracking on Cooling to $-180^{\circ}\text{C}$ vs. Conversion (Region A: $T \leq -40^{\circ}\text{C}$ )

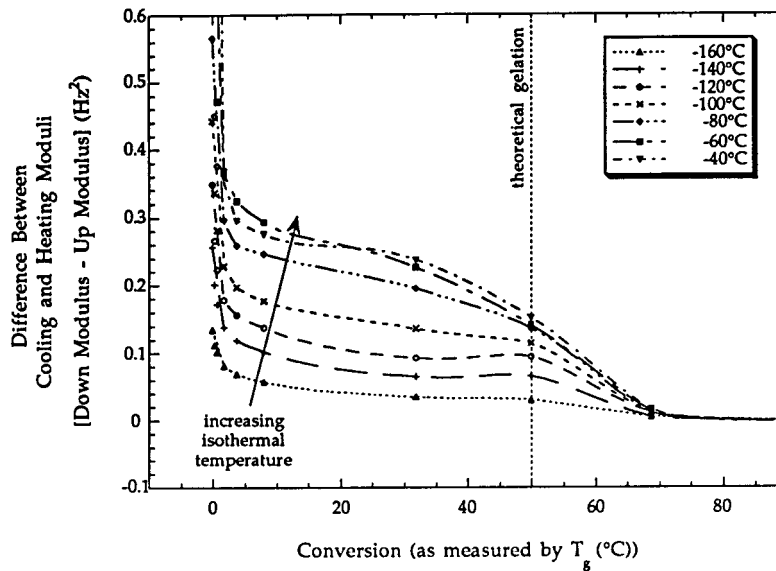


**Figure 10** Degree of further microcracking on cooling to  $-180^{\circ}\text{C}$  vs. conversion: Region A,  $T \leq -40^{\circ}\text{C}$ . The degree of further microcracking is obtained by comparing isothermal modulus data extracted from cooling and subsequent heating ramps. The theoretical gelation point,  $_{\text{gel}}T_g = 50^{\circ}\text{C}$ , is marked by a dashed line.

Observed Hysteresis in Isothermal Modulus vs. Conversion  
(Region B:  $-40^{\circ}\text{C} \leq T \leq 20^{\circ}\text{C}$ )

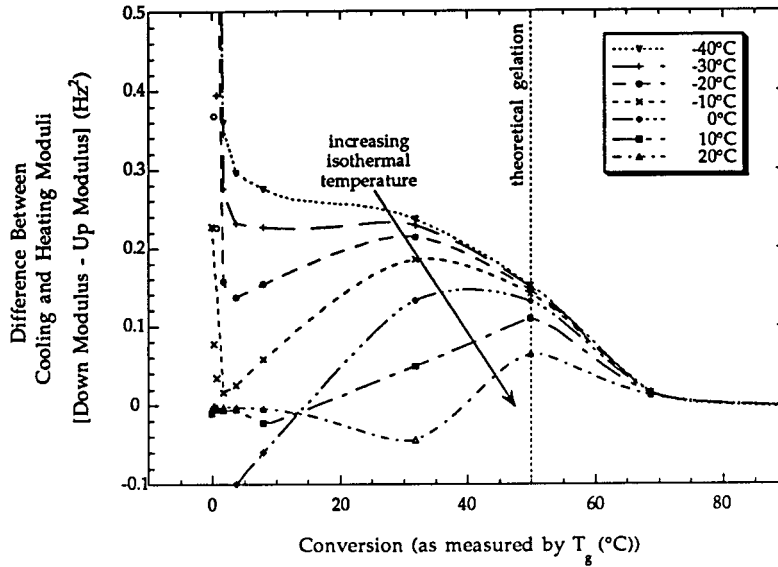


**Figure 11** Observed hysteresis in isothermal modulus vs. conversion: Region B,  $-40^{\circ}\text{C} \leq T \leq 20^{\circ}\text{C}$ . The observed hysteresis is measured using the difference between isothermal modulus data extracted from cooling ramps and subsequent heating ramps. The theoretical gelation point,  $_{gel}T_g = 50^{\circ}\text{C}$ , is marked by a dashed line.

Conversion-Temperature-Hysteresis Diagram

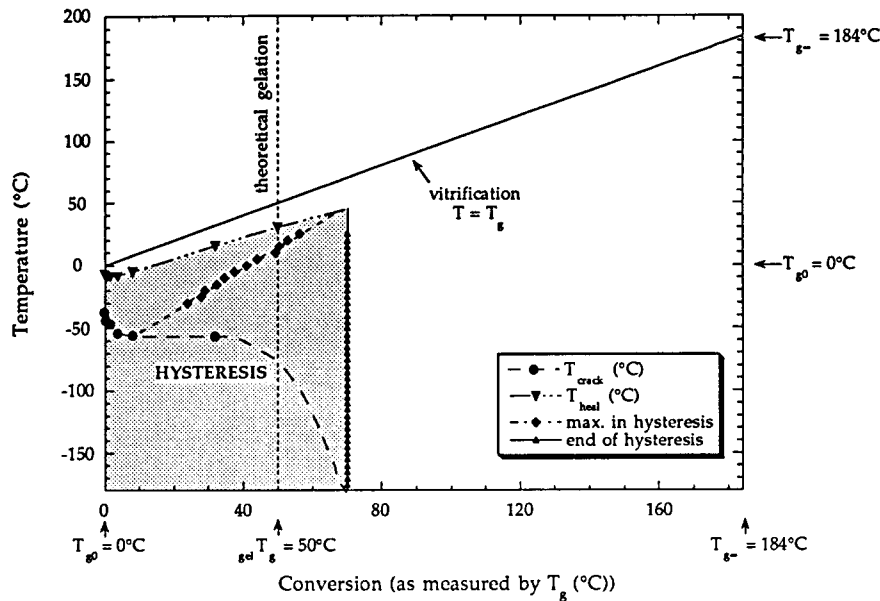


**Figure 12** Conversion-temperature-hysteresis diagram. The region of hysteresis (shaded) is defined by ( $\nabla$ ) the boundary of the healing temperature on heating and ( $\blacktriangle$ ) the end of hysteresis corresponding to a conversion of  $T_g \approx 70^{\circ}\text{C}$ . The temperatures ( $\bullet$ ) of the onset of microcracking on cooling and ( $\blacklozenge$ ) of the maximum in hysteresis are also shown.



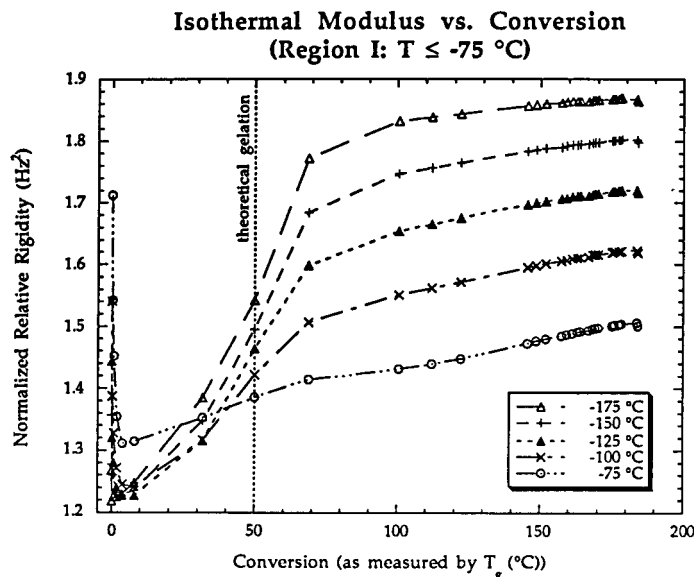


**Figure 13** Isothermal modulus vs. conversion: Region I:  $T \leq -75^\circ\text{C}$ . Data were extracted from TBA cooling ramps. Relative rigidity data were normalized so that the fully cured specimen at  $25^\circ\text{C}$  had the value 1. After a sharp initial decline, the isothermal modulus for a particular temperature increases with conversion. Note that the slope of the increase changes at  $T_g \approx 70^\circ\text{C}$ . The slope change may correspond to macroscopic gelation. The vertical line represents the value of the glass transition temperature at the theoretical gelation point,  ${}_{\text{gel}}T_g = 50^\circ\text{C}$ .

flow of material along the glass braid substrate at temperatures above  $T_g$ .<sup>6</sup> This flow results in a dimensional change of the specimen which manifests itself as a decrease in the relative rigidity. At higher conversions (after the sharp initial decline), the isothermal modulus for a particular temperature increases with conversion. Note that the slope of the increase changes at  $T_g \approx 70^\circ\text{C}$ . The slope change may correspond to macroscopic gelation. Note that the theoretical gelation point at  ${}_{\text{gel}}T_g \approx 50^\circ\text{C}$  is marked by a vertical line in Figure 13.

In the second temperature region, Region II:  $-75^\circ\text{C} \leq T \leq T_{g0}$ , the material is always below the initial glass transition temperature ( $T_{g0} = 0^\circ\text{C}$ ) and thus is glassy; however, since the material is not as deep in the glassy state as in Region I, the material behavior is somewhat different. The glass transition, while reported as a single temperature, actually exists as a temperature range. Previous studies have estimated that the glass transition region extends approximately  $40^\circ\text{C}$  on either side of the glass transition temperature as measured. Thus, the glass transition may play a role in this region even though temperature is below the assigned glass transition tempera-

ture. The  $\beta$ -transition, which increases in both temperature and intensity with increasing conversion, also operates in this temperature region and may affect property behavior. Figure 14 displays the isothermal data extracted from cooling ramps for several different temperatures in Region II vs. conversion. The isothermal modulus vs. conversion behavior for Region II can be divided into several different conversion zones. At very low conversions, a drop in the isothermal modulus similar to that seen in Region I is observed for all but the  $0^\circ\text{C}$  curve. As discussed above, this drop may be due to an artifact of the experiment. Any flow of the material on the supporting braid results in a dimensional loss of material which appears as a decrease in relative rigidity in the glassy state.<sup>6</sup> (This is not apparent in the rubbery or liquid states where the relative rigidity parameter is dominated by the glass fiber substrate.) The  $0^\circ\text{C}$  curve is initially on the glass transition (with a low modulus), so the argument that the relative rigidity parameter is dominated by the glass substrate explains the lack of a decrease in the modulus at  $0^\circ\text{C}$ . At slightly higher conversions, the modulus increases with increasing  $T_g$  and passes through a maximum (with the

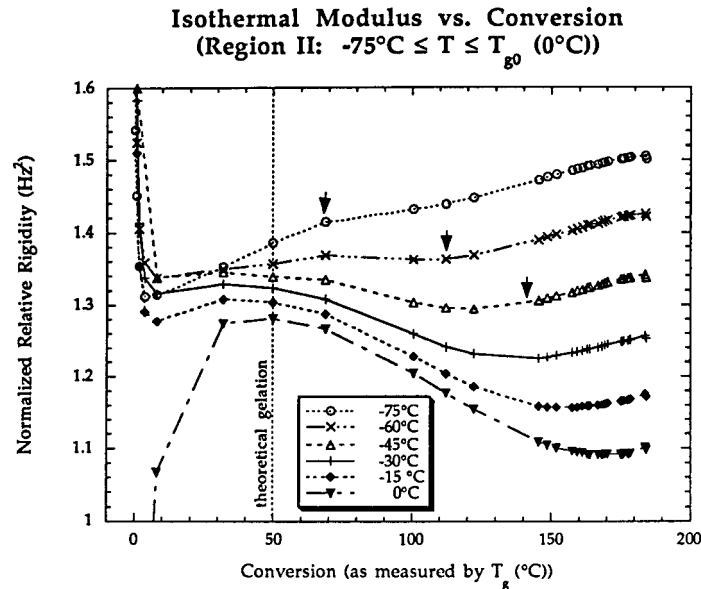


**Figure 14** Isothermal modulus vs. conversion: Region II:  $75^{\circ}\text{C} \leq T \leq T_{g0} (0^{\circ}\text{C})$ . Data were extracted from TBA cooling ramps. Relative rigidity data were normalized so that the fully cured specimen at  $25^{\circ}\text{C}$  had the value 1. After a sharp initial decline, the isothermal modulus for a temperature in the middle of the region increases with conversion to a maximum, then decreases to a minimum. Vertical arrows correspond to the conversion at which the  $\beta$ -transition equals the isothermal temperature. The dashed vertical line corresponds to theoretical gelation,  $_{gel}T_g = 50^{\circ}\text{C}$ .

exception of the  $-75^{\circ}\text{C}$  data which lie on the boundary between Regions I and II). The maximum in the isothermal modulus is considered to result from competition between a process which increases the modulus with a process which decreases the modulus. A similar maximum occurs in Region III.

Discussion of possible explanations for the maximum and the “anomaly” (the decrease in the isothermal modulus with increasing conversion) follows later. With further increasing conversion, the modulus decreases to a minimum and then increases at high conversions (again, the  $-75^{\circ}\text{C}$  data do not behave in this manner). Note that the vertical arrows in Figure 14 represent the conversions at which the  $\beta$ -transition temperature has its value equal that of the isothermal curve beneath the arrow: data to the left of the arrow correspond to  $T_{\beta} < T$ , whereas data to the right of the arrow corresponds to  $T_{\beta} > T$ . Similar minima occur in part of Region III.

Above the glass transition temperature, Region III:  $T \geq T_{g0}$ , the material is liquid or rubbery depending on the conversion. When the glass transition temperature rises through the isothermal temperature of measurement, the material

vitrifies and thus the modulus can increase by more than an order of magnitude. This effect of the rise of the glass transition temperature can be seen in Figure 15, which shows the isothermal modulus extracted from cooling ramps vs. conversion for several temperatures in Region III. The vertical arrows in Figure 15 mark the conversion at which the isothermal temperature immediately beneath the arrow is equal to the glass transition temperature. Note that this point falls somewhat less than midway through the rise in modulus due to vitrification. After the steep climb in the modulus attributed to vitrification, the modulus passes through a maximum, after which the modulus decreases with conversion. This decrease in the modulus with conversion is termed “anomalous” since the modulus might be expected to increase with the increased conversion as a consequence of the decrease in the specific volume which is associated with the process of a cure. Note that a subsequent minimum is observable at high conversions in some of the isothermal curves. This minimum may be related to the minimum seen in Region II. The minimum with respect to both regions is discussed later.

The conversion–temperature–property dia-

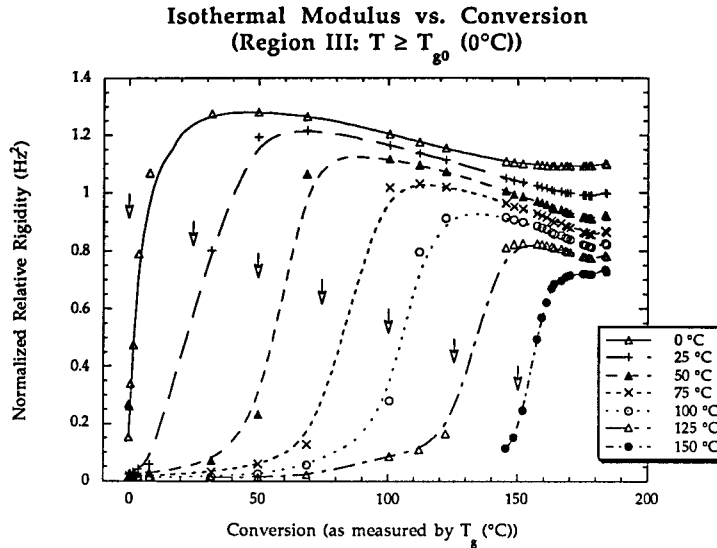


**Figure 15** Isothermal modulus vs. conversion: Region III:  $T \geq T_{g0}$  ( $0^\circ\text{C}$ ). Data were extracted from TBA cooling ramps. Relative rigidity data were normalized so that the fully cured specimen at  $25^\circ\text{C}$  had the value 1. As  $T_g$  rises to the temperature of measurement, the material vitrifies, resulting in a sharp increase in the modulus. Vertical arrows correspond to the point at which  $T_g$  equals the isothermal temperature of measurement (i.e., vitrification). After vitrification, the modulus passes through a maximum. The subsequent decrease in the modulus with conversion is termed the “anomaly.” At very high conversions, the modulus passes through a minimum and appears to increase slightly.

gram format was also used to summarize transition and isothermal modulus data (from cooling data) for the DGEBA–TMAB system (Fig. 16). The evolution of the following transitions with increasing conversion,  $T_g$ , is shown: the glass transition,  $T_g$ , the  $\gamma$ -transition,  $T_\gamma$ , the  $\beta$ -transition,  $T_\beta$ , and the liquid–liquid transition,  $T_{ll}$ . The diagram can be used horizontally or vertically for transitions. Three sets of modulus data are shown: the maximum in the isothermal modulus, the minimum in the isothermal modulus, and a slope change in the isothermal modulus. The diagram defines the regions of isothermal modulus behavior. The patterned shaded region corresponds to the “anomaly” where the isothermal modulus decreases with increased conversion. Note that the maximum and minimum in the isothermal modulus data have been extrapolated to join the slope change data to bound the “anomalous” region. The isothermal modulus increases with increased conversion in unshaded areas. The modulus data must be read isothermally. A horizontal reading represents the isothermal consequence of the cure. For example, reading across horizontally at  $30^\circ\text{C}$ , the material will first pass

through the liquid–liquid transition at  $T_g \approx 20^\circ\text{C}$ ; then when  $T_g = 30^\circ\text{C}$ , the material has vitrified, and later when  $T_g = 50^\circ\text{C}$ , it has gelled (theoretically), and at  $T_g \approx 80^\circ\text{C}$ , the isothermal modulus passes through a maximum. A vertical reading corresponds to temperature change at a fixed conversion. Reading the diagram vertically starting from  $-180^\circ\text{C}$  with material for which  $T_g = 60^\circ\text{C}$ , the material will pass through three transitions on heating: the  $\beta$ -transition,  $T_\beta$ ; the glass transition,  $T_g$ ; and, finally, the liquid–liquid transition,  $T_{ll}$ . The dashed vertical line corresponds to the glass transition temperature at theoretical gelation,  $_{gel}T_g = 50^\circ\text{C}$ .

A maximum was observed in the Regions II and III plots of the isothermal modulus extracted from cooling data vs. conversion. Other studies of the water absorption, density, and free volume of various thermosetting epoxies revealed similar counterintuitive (thus “anomalous”) results. Aronhime et al. reported an increase in isothermal water absorption with increasing cure.<sup>7</sup> It might have been expected that water absorption would monotonically decrease with increasing conversion since the increased crosslinking might be pre-

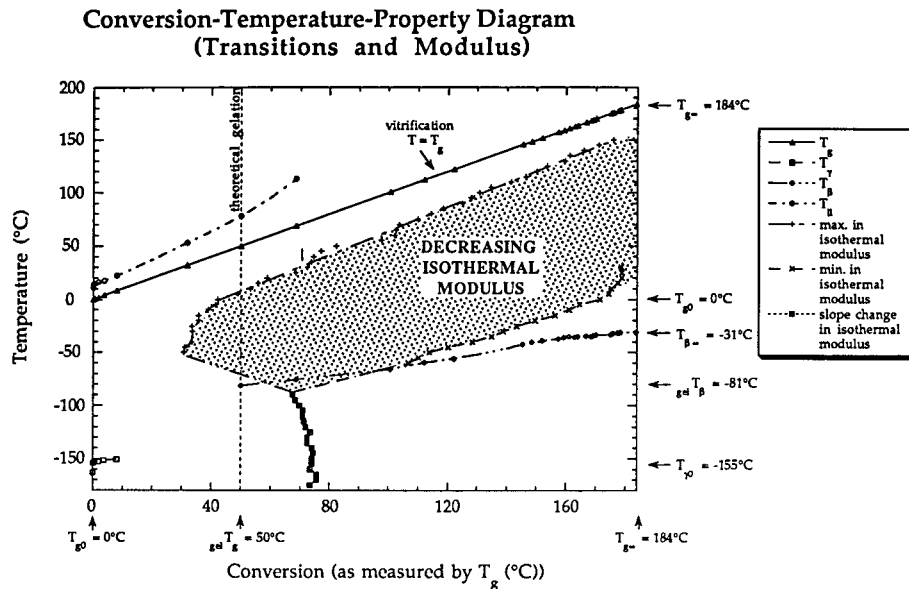


**Figure 16** Conversion–temperature–property diagram for transitions and isothermal modulus. The evolution of the following transitions with increasing conversion,  $T_g$ , is shown: the glass transition,  $T_g$ ; the  $\gamma$ -transition,  $T_\gamma$ ; the  $\beta$ -transition,  $T_\beta$ ; and the liquid–liquid transition,  $T_l$ . The diagram can be used horizontally or vertically for transitions. The dashed vertical line corresponds to the glass transition temperature at theoretical gelation,  $_{gel}T_g = 50^\circ\text{C}$ . Three sets of modulus data are shown: the maximum in isothermal modulus, the minimum in isothermal modulus, and a slope change in isothermal modulus. The diagram thereby defines the regions of isothermal modulus behavior. The shaded region corresponds to the “anomaly” where the isothermal modulus decreases with increased conversion. Note that the modulus data can only be read isothermally (horizontally).

sumed to result in increased density due to a lower free volume which would translate into less space for water to occupy. Pang and Gillham found that the isothermal density of an epoxy system passed through a maximum, after which the density decreased with increasing conversion.<sup>8</sup> This result, in addition to the work by Aronhime et al. on water absorption, indicated that the assumption that free volume decreases monotonically with conversion was questionable. The assumption that the free volume of the system would decrease is based on an argument involving the free volume associated with chain ends. During the cure of a thermosetting polymeric material, chain ends are consumed by the reaction; thus, the free volume associated with chain ends should decrease. Consequently, on this basis, the overall free volume of the polymer would decrease, resulting in a decrease in the specific volume of the material since the specific volume is the sum of the occupied volume and free volume. This argument assumes that the only change in

the overall free volume of the system is associated with the chain ends. However, consideration of the occupied volume, as calculated from the summation of van der Waal’s volumes of the constituent atoms and their bonding, leads to the occupied volume increasing with increasing conversion as a consequence of the ring opening of the epoxy groups on reaction.<sup>9</sup>

A similar investigation of a thermosetting difunctional dicyanate ester to network polycyanurate showed that, like the epoxy system, the specific volume passes through a minimum with increasing conversion,<sup>6</sup> but, unlike the epoxy system, the occupied volume as calculated from the summation of the van der Waal’s contributions of the atoms leads to a decrease in the occupied volume mainly as a consequence of the formation of triazine rings during the polymerization.<sup>9</sup> Similar macroscopic changes in the specific volume and the dissimilar changes in the occupied volume of the epoxy and cyanate ester systems on polymerization led to the conclusion that another

factor, associated with the unoccupied free volume, is responsible for the macroscopic volume increasing with increased conversion.<sup>9</sup> Venditti et al. measured the isothermal overall free volume of the balanced stoichiometric DGEBA/TMAB system using positron annihilation spectroscopy.<sup>9</sup> The overall free volume was found to pass through a minimum, the conversion at which corresponded to maxima in modulus and density. It has been suggested that the free volume can expand on account of decreasing packing ability of the occupied volume with increasing conversion.<sup>9</sup>

The maximum in the isothermal modulus with conversion is included in the conversion–temperature–property diagram in Figure 16. Previous work on the balanced stoichiometric DGEBA/TMAB system similarly reported a maximum.<sup>4,5</sup> The proximity of the maximum to the vitrification process and thus to the glass transition suggests that the phenomena are related. The horizontal interval between the vitrification line and the data corresponding to the maximum decreases with increased conversion. It was previously discussed that the glass transition is a range rather than a single temperature. The range is not the same width at all conversions. It has been noted from the TBA raw data vs. temperature that the loss peak associated with the glass transition temperature is broader at intermediate conversions than it is at low and at high conversions. The change of the interval between the glass transition temperature and the maximum in the isothermal modulus with conversion is probably a reflection of the width of the glass transition temperature. The maximum, which is considered to result from a competition between a process which increases the modulus with a process that decreases the modulus, could disappear when the influence of the glass transition, or vitrification, which increases the modulus, disappears. Previous researchers in our laboratory have explained the maximum as a competition between the vitrification process (i.e., the glass transition temperature rising through the temperature of measurement) and decreased packing ability associated with the developing molecular structure. (Kinetic aspects have also been considered.<sup>8</sup>) As more crosslinks form, the growing network structure may actually require more space than material which is less reacted because of steric factors such as those associated with the crosslinking sites themselves. At low conversions, the position of the maximum deviated from the otherwise linear

shape of the data. Venditti et al. suggested that this change in shape was associated with gelation and considered that the maximum did not occur prior to gelation.<sup>5</sup> This reasoning suggests a macroscopic gelation point at a conversion that is lower than the theoretical point and thus seems unreasonable. The apparent deviation of the low conversion maximum in the isothermal modulus data may indicate that it is a separate process. The “deviant” data corresponds to Region II of the isothermal modulus behavior, in which the material is in the glassy state for all conversions. The “deviant” data may represent the point (conversion) at which the network reaches a critical point, where the packing density decreases with increasing conversion due to steric hindrance.

At relatively high conversions, the isothermal modulus at temperatures ranging from  $-60$  to  $15^{\circ}\text{C}$  passes through a minimum. The minimum in the isothermal modulus (isothermal temperature vs. conversion of the minimum in isothermal modulus) is shown in Figure 16. Previous work by Wang and Gillham<sup>4</sup> and Venditti and Gillham<sup>5</sup> suggested that the minimum may be related to the  $\beta$ -transition. The  $\beta$ -transition temperature vs. conversion is also shown in Figure 16. The minimum does not appear to lie directly on the  $\beta$ -transition vs. conversion data, but an argument similar to that used to relate the glass transition temperature to the maximum in the isothermal modulus may aid in an understanding of the relationship. The  $\beta$ -transition appears as a broad peak in the mechanical loss. The intensity and width of the peak appear to increase with increasing conversion. Using the idea that the transition temperature is a range and not a point, the minimum may represent the beginning of the influence of the  $\beta$ -transition. Since transitions are associated with molecular motion, the beginning of the influence of the  $\beta$ -relaxation at a particular temperature represents the beginning of a freezing out of a particular type of motion as the transition rises through the measurement temperature. Diminished motion may thus lead to an increased modulus, which represents a measure of the ability of the material to deform with stress.

The summary conversion–temperature–property diagram (Fig. 17) was constructed by superimposing transition, modulus, and hysteresis data. Light gray shading represents the hysteresis region, moderate patterned shading represents the “anomaly” (isothermal modulus decreases with increasing conversion), and the dark

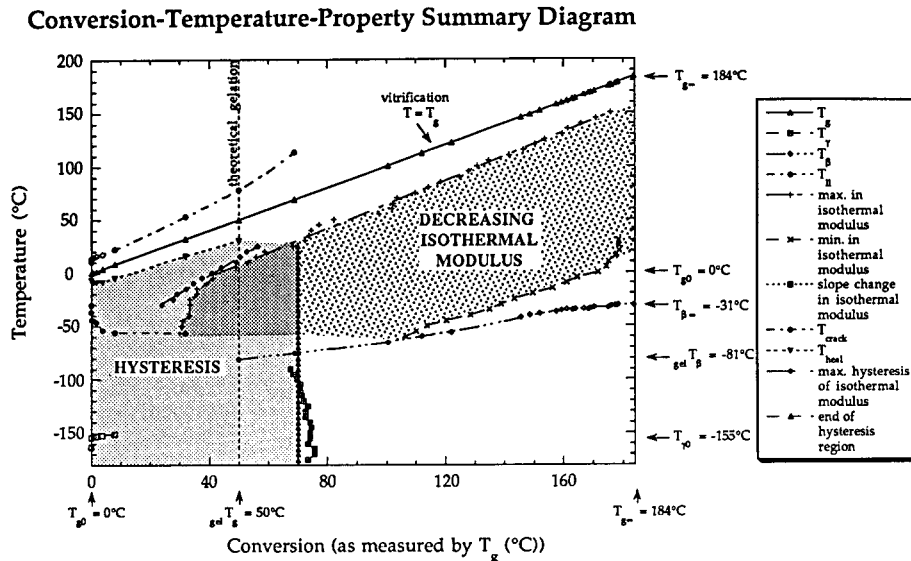


**Figure 17** Conversion–temperature–property summary diagram for the balanced stoichiometric DGEBA/TMAB system. The conversion–temperature–transition, conversion–temperature–modulus, and conversion–temperature–hysteresis diagrams have been overlaid. Light shading represents the hysteresis region (due to microcracking on cooling), moderate shading represents the “anomaly” region (isothermal modulus decreases with increasing conversion), and dark shading represents the overlap of the hysteresis and the “anomaly” regions.

gray shading represents the overlap of hysteresis and the “anomaly.” (Note that extrapolations in the conversion–temperature–hysteresis diagram (Fig. 12) and the conversion–temperature–property diagram for transitions and the modulus (Fig. 16) are not included in Figure 17. This diagram is a framework for relating macroscopic behavior such as modulus and hysteresis to discrete molecular motions (transitions) and molecular structure (conversion).

## CONCLUSIONS

The following statements represent a summary of this research on the evolving of properties with increase of cure:

- $T_{\text{crack}}$ , the temperature of the onset of microcracking on cooling, decreased with increasing conversion.
- $T_{\text{heal}}$ , the temperature of healing of microcracks on heating, is related to the glass transition temperature and, thus, increased with increasing conversion. The temperature dif-

ference between  $T_g$  and  $T_{\text{heal}}$  appears to be approximately constant.

- The maximum in hysteresis (the maximum difference between the moduli extracted from cooling and heating ramps) represents a competition between increased brittleness associated with the rise of  $T_g$  above the isothermal temperature of measurement and the increased toughness of the matrix associated with increased conversion.
- No microcracking (and thus no hysteresis) was apparent after macroscopic gelation ( $T_g \approx 70^\circ\text{C}$ ).
- The maximum in the isothermal modulus with increasing conversion is considered to arise from competition between a process which increases the modulus (vitrification,  $T_g$ ) with a process which decreases the modulus (decreased packing ability of the growing network structure).
- The minimum in the isothermal modulus with increasing conversion appears to be linked to the  $\beta$ -transition. The minimum is considered to result from the competition between a process which decreases the modulus

(decreased packing ability of the network) and the rise of the  $\beta$ -transition which freezes out particular internal motions, thus increasing the modulus.

- The region of hysteresis (microcracking) was incorporated into a conversion–temperature–property diagram which also includes transition and isothermal modulus (anomaly) information. The conversion–temperature–property diagram is a framework for relating macroscopic behavior to material transitions and structure (conversion).

## REFERENCES

1. J. K. Gillham and J. B. Enns, *Trends Polym. Sci.*, **2**, 406–419 (1994).
2. A. S. Valley, BSE Thesis, Department of Chemical Engineering, Princeton University, May 1996.
3. M. T. DeMeuse and J. K. Gillham, *J. Appl. Polym. Sci.*, **64**, 27–38 (1997).
4. X. Wang and J. K. Gillham, *J. Appl. Polym. Sci.*, **47**, 425–446 (1993).
5. R. A. Venditti and J. K. Gillham, *J. Appl. Polym. Sci.*, **56**, 1687–1705 (1995).
6. S. L. Simon and J. K. Gillham, *J. Appl. Polym. Sci.*, **51**, 1741–1752 (1994).
7. M. T. Aronhime, X. Peng, J. K. Gillham, and R. D. Small, *J. Appl. Polym. Sci.*, **32**, 3589–3626 (1986).
8. K. P. Pang and J. K. Gillham, *J. Appl. Polym. Sci.*, **37**, 1969–1991 (1989).
9. R. A. Venditti, J. K. Gillham, Y. C. Yean, and Y. Lou, *J. Appl. Polym. Sci.*, **56**, 1207–1220 (1995).
10. S. L. Maddox and J. K. Gillham, *J. Appl. Polym. Sci.*, **64**, 55–67 (1997).